

Collider probes of singlet fermionic dark matter scenarios for the Fermi gamma-ray excess

Yeong Gyun Kim^{a,*}, Chan Beom Park^{b,†}, and Seodong Shin^{c,d,‡}

^a*Department of Science Education, Gwangju National University of Education,
Gwangju 61204, Korea*

^b*Center for Theoretical Physics of the Universe,
Institute for Basic Science (IBS), Daejeon 34051, Korea*

^c*Enrico Fermi Institute, University of Chicago, Chicago, IL 60637, USA*

^d*Department of Physics and IPAP, Yonsei University, Seoul 03722, Korea*

Abstract

We investigate the collider signatures of the three benchmark points in the singlet fermionic dark matter model. The benchmark points, which were introduced previously to explain the Fermi gamma-ray excess by dark matter (DM) pair annihilation at the Galactic center, have definite predictions for future collider experiments such as the International Linear Collider and the High-Luminosity LHC. We consider four collider observables: (1) Higgs signal strength (essentially hZZ coupling), (2) triple Higgs coupling, (3) exotic Higgs decay, and (4) direct production of a new scalar particle. The benchmark points are classified by the final states of the DM annihilation process: a pair of b quarks, SM-like Higgs bosons, and new scalar particles. Each benchmark scenario has detectable new physics signals for the above collider observables that can be well tested in the future lepton and hadron colliders.

*ygkim@gnue.ac.kr

†cbpark@ibs.re.kr

‡seodongshin@yonsei.ac.kr

Contents

1	Introduction	1
2	Singlet fermionic dark matter	2
3	Benchmark points and collider signatures	4
3.1	BP I ($\psi\bar{\psi} \rightarrow b\bar{b}$ annihilation channel)	4
3.2	BP II ($\psi\bar{\psi} \rightarrow h_1 h_1$ annihilation channel)	8
3.3	BP III ($\psi\bar{\psi} \rightarrow h_2 h_2$ annihilation channel)	9
4	Conclusions	11

1 Introduction

The existence of dark matter (DM) in the universe is now well established by various experiments observing the gravitational interactions of the DM and the anisotropy of cosmic microwave background. In order to investigate its feature as a particle, it is required to observe non-gravitational interactions of DM with the standard model (SM) particles. One of such trials is indirect detections of the DM, which probe the signals from the annihilation or the decay of the DM in the current universe. They can contribute to energetic charged particles, photons, and neutrinos which are observable in satellite and terrestrial detectors. In particular, the gamma-ray signals have always drawn attention in the sense that we can identify the location of the sources. Interestingly, several independent researches have reported an excess of the gamma-ray emission from the Galactic center (GC) above the expected astrophysical background from the analysis of the Fermi Large Area Telescope (LAT) data [1–11], confirmed later by the experimental group [12].

The excess can be explained by DM annihilations or decays although the explanations by unidentified astrophysical sources still remain viable possibilities. In Ref. [13] we examined the possibility that the GeV scale Fermi gamma-ray excess at the GC can be explained by the DM annihilation in the singlet fermionic dark matter (SFDM) model [14,15]. Within the framework, we showed that the DM annihilation into a bottom-quark pair, Higgs pair, and new scalar pair can provide good fits to the Fermi gamma-ray excess data. However, due to the unknown populations of other astrophysical sources near the GC, it is very hard to confirm that the excess is originated from the DM only via the astrophysical observations in general. Hence, as a complementary approach to support the DM explanation, it is necessary to probe the relevant DM scenarios in collider experiments where the background events are relatively well controlled. Following this strategy, we investigate the detection prospects of the SFDM signals explaining the gamma-ray excess in future colliders such as the High-Luminosity Large Hadron Collider (HL-LHC) and the International Linear Collider (ILC) as reference machines of hadron and lepton colliders. Note that the analysis results in the

ILC can be easily converted to those in the Circular Electron Positron Collider (CEPC) as well.

The reference model parameters in Ref. [13] are chosen to explain the Fermi gamma-ray excess with a best fit for each annihilation channel: resonant $b\bar{b}$ production, double Higgs production, Higgs and a new scalar production when they are almost degenerate in mass, and double new scalar production. Then, we can proceed analyses with these fixed reference parameters providing definite predictions for collider phenomenology. The scenario, where the SM-like Higgs boson and the new scalar are too degenerate in mass and the couplings of the new scalar to WW and ZZ are highly suppressed, is quite hard to be probed in collider experiments. Thereby we only consider the reference parameters of the other three channels and name them benchmark point (BP) I, II, and III, in order.

This paper is organized as follows. We briefly describe the SFDM model in Sec. 2. The benchmark scenarios for explaining the Fermi gamma-ray excess are introduced and their possible collider signatures in the future collider experiments are discussed in Sec. 3. Section 4 is devoted to conclusions.

2 Singlet fermionic dark matter

In this section, we summarize the key features of the SFDM model used in explaining the gamma-ray excess from the GC [13]. The dark sector is composed of a real scalar field S and a Dirac fermion field ψ , both of which are singlet under the SM gauge group.

The Lagrangian for the dark sector is given by the following renormalizable interactions.

$$\mathcal{L}^{\text{dark}} = \bar{\psi}(i\not{\partial} - m_{\psi_0})\psi + \frac{1}{2}\partial_\mu S\partial^\mu S - g_S(\cos\theta\bar{\psi}\psi + \sin\theta\bar{\psi}i\gamma^5\psi)S - V_S(S, H), \quad (1)$$

where the singlet scalar potential is

$$V_S(S, H) = \frac{1}{2}m_0^2 S^2 + \lambda_1 H^\dagger H S + \lambda_2 H^\dagger H S^2 + \frac{\lambda_3}{3!} S^3 + \frac{\lambda_4}{4!} S^4. \quad (2)$$

As compared to the original proposal of the SFDM [14], the pseudoscalar interaction in the dark sector is further introduced to obtain a good fit to the gamma-ray excess from the GC using the DM annihilation. See Ref. [13] for the detail of the fit to the gamma-ray data.

The SM Higgs potential is given as

$$V_{\text{SM}} = -\mu^2 H^\dagger H + \lambda_0 (H^\dagger H)^2. \quad (3)$$

The Higgs doublet H is written in the unitary gauge after the electroweak symmetry breaking as follows:

$$H = \frac{1}{\sqrt{2}} \begin{pmatrix} 0 \\ v_h + h \end{pmatrix} \quad (4)$$

with $v_h \simeq 246$ GeV. The singlet scalar field also develops a nonzero vacuum expectation value, v_s , and the singlet scalar field is written as $S = v_s + s$. The mass parameters μ^2 and

m_0^2 can be expressed in terms of other parameters by using the minimization condition of the full scalar potential $V_S + V_{\text{SM}}$, *i.e.*,

$$\begin{aligned}\mu^2 &= \lambda_0 v_h^2 + (\lambda_1 + \lambda_2 v_s) v_s, \\ m_0^2 &= -\left(\frac{\lambda_1}{2v_s} + \lambda_2\right) v_h^2 - \left(\frac{\lambda_3}{2v_s} + \frac{\lambda_4}{6}\right) v_s^2.\end{aligned}\quad (5)$$

The mass terms of the scalar fields are

$$-\mathcal{L}_{\text{mass}} = \frac{1}{2}\mu_h^2 h^2 + \frac{1}{2}\mu_s^2 s^2 + \mu_{hs}^2 h s, \quad (6)$$

where

$$\begin{aligned}\mu_h^2 &= 2\lambda_0 v_h^2, \\ \mu_s^2 &= -\frac{\lambda_1 v_h^2}{2v_s} + \frac{(3\lambda_3 + 2\lambda_4 v_s)v_s}{6}, \\ \mu_{hs}^2 &= (\lambda_1 + 2\lambda_2 v_s)v_h.\end{aligned}\quad (7)$$

A non-vanishing value of μ_{hs}^2 induces mixing between the SM Higgs field configuration h and the singlet scalar field s as

$$\begin{pmatrix} h_1 \\ h_2 \end{pmatrix} = \begin{pmatrix} \cos \theta_s & \sin \theta_s \\ -\sin \theta_s & \cos \theta_s \end{pmatrix} \begin{pmatrix} h \\ s \end{pmatrix}, \quad (8)$$

The mixing angle θ_s is given by

$$\tan \theta_s = \frac{y}{1 + \sqrt{1 + y^2}} \quad (9)$$

with $y \equiv 2\mu_{hs}^2/(\mu_h^2 - \mu_s^2)$. Then, the physical Higgs boson masses are

$$m_{h_1, h_2}^2 = \frac{1}{2} \left[(\mu_h^2 + \mu_s^2) \pm (\mu_h^2 - \mu_s^2) \sqrt{1 + y^2} \right]. \quad (10)$$

We define that h_1 is the SM-like Higgs boson with $m_{h_1} = 125$ GeV and h_2 is the singlet-like scalar boson throughout this paper.

The imaginary mass term of the DM particle ψ from the pseudoscalar interaction, proportional to $\sin \theta$ in (1), can be eliminated by a chiral transformation and field redefinition, as stated in Refs. [13, 16]. Then, one can find that the DM mass is given by

$$m_\psi = \sqrt{(m_{\psi_0} + g_S v_s \cos \theta)^2 + g_S^2 v_s^2 \sin^2 \theta}. \quad (11)$$

And the dark sector Yukawa interactions are redefined as

$$-\mathcal{L}_{\text{int}}^{\text{dark}} = g_S \cos \xi s \bar{\psi} \psi + g_S \sin \xi s \bar{\psi} i \gamma^5 \psi, \quad (12)$$

where

$$\cos \xi = \frac{m_{\psi_0} \cos \theta + g_S v_s}{m_\psi},$$

$$\sin \xi = \frac{m_{\psi_0} \sin \theta}{m_{\psi}}. \quad (13)$$

Therefore, there are three independent model parameters for the singlet fermion: m_{ψ} , g_S , and ξ . On the other hand, the masses m_{h_1, h_2} , the mixing angle θ_s , and self-couplings of the two physical Higgs particles h_1 and h_2 are determined by the six independent parameters in the scalar potential, λ_0 , λ_1 , λ_2 , λ_3 , λ_4 , and v_s . For a reference, we recall that the scalar triple Higgs self-couplings c_{ijk} for $h_i h_j h_k$ interactions are expressed as

$$\begin{aligned} c_{111} &= 6\lambda_0 v_h \cos^3 \theta_s + (3\lambda_1 + 6\lambda_2 v_s) \cos^2 \theta_s \sin \theta_s + 6\lambda_2 v_h \cos \theta_s \sin^2 \theta_s + (\lambda_3 + \lambda_4 v_s) \sin^3 \theta_s, \\ c_{112} &= -6\lambda_0 v_h \cos^2 \theta_s \sin \theta_s + 2\lambda_2 v_h (2 \cos^2 \theta_s \sin \theta_s - \sin^3 \theta_s) \\ &\quad + (\lambda_1 + 2\lambda_2 v_s) (\cos^3 \theta_s - 2 \cos \theta_s \sin^2 \theta_s) + (\lambda_3 + \lambda_4 v_s) \cos \theta_s \sin^2 \theta_s, \\ c_{122} &= 6\lambda_0 v_h \cos \theta_s \sin^2 \theta_s + 2\lambda_2 v_h (\cos^3 \theta_s - 2 \cos \theta_s \sin^2 \theta_s) \\ &\quad - (\lambda_1 + 2\lambda_2 v_s) (2 \cos^2 \theta_s \sin \theta_s - \sin^3 \theta_s) + (\lambda_3 + \lambda_4 v_s) \cos^2 \theta_s \sin \theta_s, \\ c_{222} &= -6\lambda_0 v_h \sin^3 \theta_s + (3\lambda_1 + 6\lambda_2 v_s) \sin^2 \theta_s \cos \theta_s - 6\lambda_2 v_h \sin \theta_s \cos^2 \theta_s \\ &\quad + (\lambda_3 + \lambda_4 v_s) \cos^3 \theta_s. \end{aligned} \quad (14)$$

3 Benchmark points and collider signatures

We consider the three benchmark points of the SFDM model, which can explain the Fermi gamma-ray excess from the DM pair annihilations. In Ref. [13], we demonstrated in detail that the annihilation of DM into a bottom-quark pair, Higgs pair, and new scalar pair can give good fits to the Fermi-LAT gamma-ray data. Because model parameters are fixed in order to explain the Fermi gamma-ray excess, it gives rise to definite predictions for collider phenomenology. If the predictions are confirmed by the future collider experiments, the benchmark points will be strongly favored as the solution for the Fermi gamma-ray excess.

The benchmark points we consider for the collider study are classified by the final state of the main DM annihilation process. The first benchmark point corresponds to the DM annihilation channel into a bottom-quark pair (BP I), while the second and third benchmark points correspond to the DM annihilation channels into a Higgs pair (BP II) and into a new scalar pair (BP III), respectively, which subsequently decay to the SM particles. Let us now discuss the details of the three benchmark points and their collider signatures one by one.

3.1 BP I ($\psi\bar{\psi} \rightarrow b\bar{b}$ annihilation channel)

The channel of DM annihilation into a bottom-quark pair is one of the most widely considered possibilities explaining the gamma-ray excess. For example, the model independent study in Ref. [11] showed that the DM annihilation into $b\bar{b}$ gives a good fit to the gamma-ray excess data if $m_{\text{DM}} \simeq 48.7$ GeV and the DM annihilation cross section $\langle\sigma v\rangle \simeq 1.75 \times 10^{-26}$ cm³ s⁻¹ for a self-conjugate DM. In the SFDM model, this channel can give a best fit to the observed data when $m_{\psi} = 49.706$ GeV, $m_{h_2} = 99.416$ GeV, $m_{h_1} = 125.3$ GeV, and $\sin \theta_s = -0.117$ from the reference parameters $\lambda_0 = 0.128816$, $\lambda_1 = 36.625338$ GeV, $\lambda_2 = -0.131185$, $\lambda_3 = -333.447606$ GeV, $\lambda_4 = 5.648618$, $v_s = 150.017297$ GeV, $g_S = 0.055$, and $\sin \xi = 0.01$ [13]. With the parameter setup, we obtain the correct DM relic density $\Omega h^2 = 0.118$, and the DM

annihilation cross section $\langle\sigma v\rangle = 1.5 \times 10^{-26} \text{ cm}^3 \text{ s}^{-1}$ which can explain the Fermi gamma-ray excess within the uncertainty of the galaxy halo profile near the GC. Note, however, that only a narrow parameter region around the resonance of $\psi\bar{\psi} \rightarrow b\bar{b}$ is allowed to fit the correct relic density and the new scalar h_2 needs to be almost scalar in the dark sector, *i.e.*, $\sin\xi = 0.01$, to avoid the strong astrophysical bounds from the observation of the gamma-rays coming from the dwarf spheroidal galaxies by Fermi-LAT [17] and the antiproton ratio by PAMELA [18] and AMS-02 [19]. On the other hand, the small mixing angle between the SM Higgs and the singlet scalar, *i.e.*, $\sin\theta_s = -0.117$ suppresses the spin-independent cross section of the DM recoiling against nucleon as $\sim 6.3 \times 10^{-48} \text{ cm}^2$, which is below the constraints from various DM direct detection experiments. In the following subsections, we discuss the collider signatures of this benchmark point in terms of the Higgs signal strength, triple Higgs coupling, exotic Higgs decays, and direct production of h_2 .

3.1.1 Higgs signal strength

As already mentioned, the physical Higgs states are admixtures of h and s in the SFDM model. Therefore, the SM-like Higgs couplings to SM gauge bosons and fermions are universally suppressed by the factor of $\cos\theta_s$, compared to the couplings in the SM.

The universal reduction factor $\cos\theta_s$ can be precisely measured at the ILC. The SM cross section for the Higgsstrahlung process $e^+e^- \rightarrow Zh$ reaches its maximum value at $\sqrt{s} = 250 \text{ GeV}$. About a half million Zh events are expected from the integrated luminosity of 2 ab^{-1} with a suitable polarization of e^+e^- beams. Then, it is possible to precisely measure the inclusive cross section of the Higgsstrahlung process using the recoil mass technique, which disregards the decay products of the Higgs boson. For a Z boson decaying into a pair of fermions, $Z \rightarrow f\bar{f}$, the recoil mass is defined as [20, 21]

$$M_{\text{recoil}} = \sqrt{s - 2\sqrt{s}(E_f + E_{\bar{f}}) + m_{f\bar{f}}^2}. \quad (15)$$

It corresponds to the mass of the Higgs boson associated with the Z boson in the Higgsstrahlung process. On the other hand, the simplest approach to represent the effect of new physics is the so-called κ formalism, where the form of Higgs interactions to the SM particles are the same as the SM, but the couplings are rescaled from the SM value. In the SFDM model, the cross section σ_{Zh_1} is proportional to $\cos^2\theta_s$. The $\cos\theta_s$ value can be determined very precisely, with accuracy of 0.38% assuming a total integrated luminosity of 2 ab^{-1} in the κ formalism:

$$\kappa_Z^2 = \frac{\sigma(e^+e^- \rightarrow Zh_1)}{\sigma(e^+e^- \rightarrow Zh)} = \cos^2\theta_s, \quad (16)$$

where the denominator is the SM prediction. Higher energy stages of the ILC experiments will reach an accuracy of 0.3% for the hZZ coupling [22].¹

The mixing angle $\sin\theta_s = -0.117$ of the BP I implies 0.7% deviation of the hZZ coupling from the SM value. Therefore the ILC experiment will be able to measure the

¹ Furthermore, it is expected that the FCC-ee experiments at 240 GeV (5 ab^{-1}) and at 365 GeV (1.5 ab^{-1}), combined with measurements of single and double Higgs processes at the HL-LHC, can achieve $\sim 0.25\%$ of the accuracy for hZZ coupling [23].

deviation. On the other hand, the HL-LHC experiment is expected to have an accuracy of $\sim 4\%$ [24, 25], which is insensitive to the deviation of the Higgs coupling.

3.1.2 Triple Higgs coupling

Another possible deviation from the SM couplings comes from the triple Higgs self-coupling c_{111} . In the SFDM model, the Higgs self-couplings are given by Eq. (14). The prospects for measuring the Higgs self-coupling is not so promising at the LHC, even at the HL-LHC. Only $\mathcal{O}(1)$ accuracy is expected for the triple Higgs coupling c_{111} from the observation of the Higgs pair production in the channel $hh \rightarrow b\bar{b}\gamma\gamma$ at the HL-LHC [26]. Meanwhile, projections for 100 TeV pp colliders show that a very good precision on the determination of the triple Higgs coupling, a statistical precision of the order of 4%, is achievable using the $b\bar{b}\gamma\gamma$ channel with the integrated luminosity of 30 ab^{-1} [27, 28]. For the BP I, the triple Higgs coupling c_{111} is 183.95 GeV, which corresponds to 3.9% reduction from the SM value, so it is on the sensitivity limit of the 100 TeV pp collider.

As for the ILC, high-energy machines with center-of-mass energies above 350 GeV can provide the opportunity of directly probing the coupling c_{111} through Higgs-pair production processes, in particular, the double Higgsstrahlung $e^+e^- \rightarrow Zh_h$ and WW -fusion $e^+e^- \rightarrow \nu\bar{\nu}hh$ processes. It is known that the interference between diagrams with and without a triple Higgs vertex has opposite sign in double Higgsstrahlung and WW -fusion, so that a combination of double Higgsstrahlung and WW -fusion measurements could be used to maximize the precision for the deviation of the triple Higgs coupling. ILC runs at 500 GeV or higher energies maximize the overall precision allowing for a determination of c_{111} with a $\sim 20\%$ uncertainty at 68% C.L. [23]

3.1.3 Exotic Higgs decays

As mentioned in Subsec. 3.1.1, the ILC can measure the absolute size of the inclusive Higgs production cross section $\sigma(e^+e^- \rightarrow Zh_1)$ by applying the recoil mass technique, which is independent of the Higgs decay modes. The recoil mass technique is applicable even if the Higgs decays invisibly and hence indispensable for extracting the Higgs branching ratio. For the sensitivity to invisible decay modes of the Higgs boson, the 250 GeV ILC with 2 ab^{-1} luminosity and polarized beams would provide an upper limit $\text{BR}(h \rightarrow \text{invisible}) < 0.3\%$ at 95% C.L. [29], which is a factor of 20 below the expected sensitivity of the HL-LHC [24, 30].

The SFDM model can lead to new Higgs decay channels if kinematically allowed. In the BP I, the mass of the singlet fermion is $m_\psi \simeq 50 \text{ GeV}$ so that the SM-like Higgs h_1 can decay into a pair of DM particles, which will escape the detector without leaving tracks, thus leading to an invisible Higgs decay. The branching ratio of the invisible Higgs decay is predicted to be $\text{BR}(h_1 \rightarrow \psi\bar{\psi}) = 0.73\%$. Hence, we expect that the invisible Higgs decay of the BP I is within the reach of the ILC, while it is beyond the reach of the HL-LHC.

3.1.4 Production of h_2 at colliders

The new particles can be produced at colliders, thus enabling a direct probe of the SFDM model through dedicated search channels. The search for the light additional Higgs boson h_2

($m_{h_2} < m_{h_1}$) directly produced via the gluon-gluon fusion process at hadron colliders suffers from a huge amount of backgrounds if $h_2 \rightarrow b\bar{b}$ is the dominant decay mode. Nevertheless, the LHC increases the sensitivity on the search for the light Higgs by combining with the other production channels. For instance, the CMS collaboration studied a low-mass resonance in the diphoton channel by combining the 8 TeV and 13 TeV data [31]². The analysis result sets the upper limit to the ratio of the production cross sections as

$$\frac{\sigma(pp \rightarrow h_2 \rightarrow \gamma\gamma)}{\sigma(pp \rightarrow h \rightarrow \gamma\gamma)_{\text{SM}}} = \sin^2 \theta_s \lesssim 0.25 \quad (17)$$

at 95% C.L. for $m_{h_2} = m_h \simeq 99$ GeV. For the HL-LHC, we expect that the upper limit will be improved by order of magnitude, $\sin^2 \theta_s \lesssim \mathcal{O}(0.01)$, so that the production of h_2 can be marginally discovered.

The strongest bound on $\sin^2 \theta_s$ from the direct production of h_2 still comes from LEP. The LEP experiments provide the 95% C.L. upper bound on the Higgs mixing angle $\sin^2 \theta_s$ as a function of the light Higgs mass m_{h_2} , which corresponds to $\sin^2 \theta_s \simeq 0.01$ for $m_{h_2} = 20$ GeV and $\sin^2 \theta_s \simeq 0.1$ for $m_{h_2} = 100$ GeV [33].

The bounds from the ILC experiment can significantly supersede the LEP bounds due to the higher luminosity by a factor of a thousand as well as polarized beams. The main production processes for light Higgs bosons at the ILC are Higgsstrahlung ($e^+e^- \rightarrow Zh_2$) for small center-of-mass energies and WW -fusion ($e^+e^- \rightarrow \nu\bar{\nu}h_2$) for large center-of-mass energies. By using MadGraph 5 [34], we obtain the production cross sections of $e^+e^- \rightarrow Zh_2$ and $e^+e^- \rightarrow \nu\bar{\nu}h_2$ for polarized beam $P(e^-, e^+) = (-80\%, +30\%)$. Fig 1 shows the cross sections at various center-of-mass energies.

Here we concentrate on the ILC run at $\sqrt{s} = 250$ GeV and apply the nominal results in Ref. [35] for the 250 GeV with the integrated luminosity 2000 fb^{-1} , which are extrapolated from the LEP results with the beam polarization $P(e^-, e^+) = (-80\%, +30\%)$. Two approaches, ‘ILC traditional’ and ‘ILC recoil’, are studied for estimating the sensitivity of the ILC to light Higgs masses. In the ILC traditional method, the signal process is identified with light Higgs decay $h_2 \rightarrow b\bar{b}$ and Z boson decay $Z \rightarrow \mu^+\mu^-$. On the other hand, in the ILC recoil method, only Z boson decay ($Z \rightarrow \mu^+\mu^-$) is exploited and the recoil mass distribution is studied. The 95% C.L. upper limits on the Higgs mixing angle $\sin^2 \theta_s$ are obtained for small Higgs masses below 125 GeV as follows [35]:

$$\sin^2 \theta_s \in [0.001, 0.002] \quad \text{with ILC traditional,} \quad (18)$$

$$\sin^2 \theta_s \in [0.003, 0.005] \quad \text{with ILC recoil.}^3 \quad (19)$$

For $m_{h_2} = 99.4$ GeV, the corresponding maximal reach at the ILC is $\sin^2 \theta_s \simeq 0.0015$. Therefore, the signal of the light Higgs h_2 can be well discovered in the case of the BP I, where $\sin^2 \theta_s = 0.014$.

²See also Ref. [32] and the references therein.

³See Ref. [36] for a more conservative estimation.

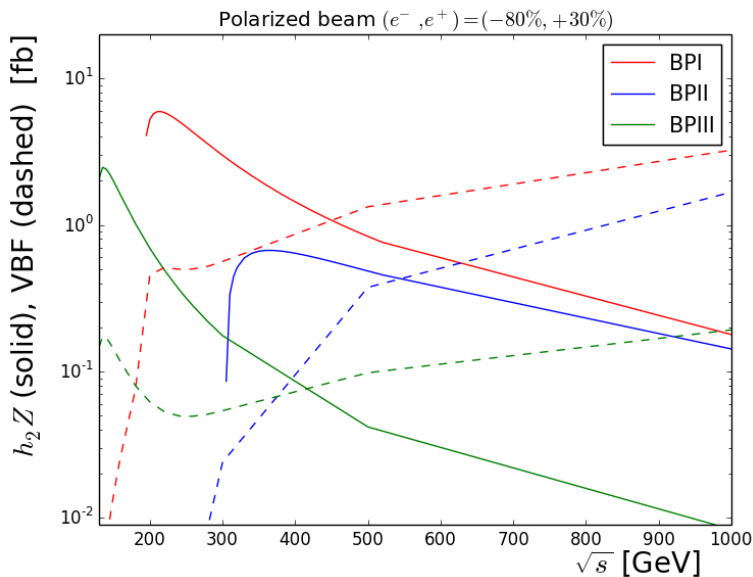


Figure 1: The production cross sections for h_2 at various \sqrt{s} in GeV with polarized beams. The solid curves correspond to the Higgsstrahlung process $e^+e^- \rightarrow Zh_2$, and the dashed curves are the WW -fusion process $e^+e^- \rightarrow \nu\bar{\nu}h_2$. The red, blue, and green colors denote the BP I, II, and III, respectively.

3.2 BP II ($\psi\bar{\psi} \rightarrow h_1h_1$ annihilation channel)

The channel of DM annihilation into the SM Higgs pair (h_1h_1 in the SFDM) is an alternative possibility explaining the gamma-ray excess. For example, a model independent study in Ref. [11] also showed that the DM annihilation into the Higgs pair gives a good fit to the gamma-ray excess data if $m_{\text{DM}} \simeq m_{h_1} \simeq 125.7$ GeV and the DM annihilation cross section $\langle\sigma v\rangle \simeq 5.33 \times 10^{-26} \text{ cm}^3 \text{ s}^{-1}$ for a self-conjugate DM.

In the SFDM model, this channel gives a best fit when $m_\psi = 127.5$ GeV, $m_{h_1} = 124.9$ GeV, $m_{h_2} = 213.5$ GeV, and $\sin\theta_s = -0.11$ from the Lagrangian parameters $\lambda_0 = 0.1315$, $\lambda_1 = 1237.8$ GeV, $\lambda_2 = -2.0$, $\lambda_3 = -820.5$ GeV, $\lambda_4 = 9.39$, $v_s = 306.15$ GeV, $g_S = 0.098$, and $\sin\xi = 1$ [13]. From these parameters, we obtain the correct DM relic density $\Omega h^2 = 0.12$, and DM annihilation cross section $\langle\sigma v\rangle = 2.11 \times 10^{-26} \text{ cm}^3 \text{ s}^{-1}$, explaining the gamma-ray excess within the uncertainty of the galaxy halo profile near the GC. Note that the BP II is safe from various astrophysical bounds even when the light Higgs h_2 is purely pseudoscalar in the dark sector. In the following subsections, we discuss the collider signatures of this benchmark point.

3.2.1 Higgs signal strength

In the BP II, the Higgs mixing angle is $\sin\theta_s = -0.11$, *i.e.*, $\cos\theta_s = 0.994$, which implies a 0.6% deviation of hZZ coupling from the SM value. As commented in the previous subsection, the deviation is within the reach of the 250 GeV ILC (0.38%).

3.2.2 Triple Higgs coupling

The triple Higgs coupling $c_{111} = 148.96$ GeV of the BP II corresponds to 22% deviation from the SM value. The deviation can be marginally detected at the ILC with higher center-of-mass energy whose accuracy is expected to be $\sim 20\%$ [23]. On the other hand, it can be well measured in the 100 TeV pp collider where $\sim 4\%$ accuracy might be reachable [24, 25].

3.2.3 Exotic Higgs decays

Since $m_{h_2} > m_{h_1}$ and $2m_\psi > m_{h_1}$, exotic Higgs decays such as $h_1 \rightarrow h_2 h_2$ and $h_1 \rightarrow \psi\bar{\psi}$ are not expected for the BP II.

3.2.4 Production of h_2 at colliders

The singlet-like Higgs mass of the BP II is $m_{h_2} = 213.5$ GeV. For the mass region of $m_{h_1} < m_{h_2} < 2m_{h_1}$, h_2 dominantly decays to the pairs of WW and ZZ . The corresponding branching ratios are $\text{BR}(h_2 \rightarrow WW) = 71.5\%$ and $\text{BR}(h_2 \rightarrow ZZ) = 28.0\%$ and the total decay width of the h_2 is about 25 MeV. The strongest constraint for the additional Higgs in this mass range comes from the current LHC searches for a new scalar resonance decaying to a pair of Z bosons [37–39]. The 95% C.L. upper bound on $\sigma(pp \rightarrow X \rightarrow ZZ)$ at the LHC with an integrated luminosity of $\sim 36 \text{ fb}^{-1}$ at the center-of-mass energy of 13 TeV, is about 2.8×10^{-1} pb for $m_X \simeq 210$ GeV. That can be translated to the upper bound on the Higgs mixing angle $\sin^2 \theta_s \lesssim 0.06$ for $m_H \simeq 210$ GeV. At the HL-LHC with integrated luminosity of 3000 fb^{-1} , an order of magnitude improvement on the bound, $\sin^2 \theta_s \lesssim 0.008$ at 95% C.L., is expected [40]. Therefore, we expect that the corresponding signal of h_2 with the mixing angle $\sin^2 \theta_s = 0.012$ can be observed at the HL-LHC.

3.3 BP III ($\psi\bar{\psi} \rightarrow h_2 h_2$ annihilation channel)

Another viable scenario for the Fermi gamma-ray excess is the DM annihilation process into dark sector particles. The scenario is the most promising channel explaining the gamma-ray excess in the sense that it is rather easy to avoid various bounds from colliders and astrophysical observations. The model independent study in Ref. [41] shows that the DM annihilation into a pair of new scalars ($\phi\phi$), each of which decays to a b -quark pair, can provide a good fit to the Fermi gamma-ray excess data. The best-fit is obtained for $m_{\text{DM}} \simeq 65$ GeV, the new scalar mass is about the half of the DM mass $m_\phi = m_{\text{DM}}/2$, and DM annihilation cross section $\langle\sigma v\rangle \simeq 2.45 \times 10^{-26} \text{ cm}^3 \text{ s}^{-1}$, assuming a self-conjugate DM.

In Ref. [13], it was shown that the above scenario can be realized in the SFDM model framework with the model parameters as follows. In the SFDM, a best fit to the excess is obtained when $m_\psi = 69.2$ GeV, $m_{h_1} = 125.1$ GeV, $m_{h_2} = 35.7$ GeV and $\sin \theta_s = 0.025$ from the parameters in the Lagrangian $\lambda_0 = 0.13$, $\lambda_1 = 4.5$ GeV, $\lambda_2 = -0.0055$, $\lambda_3 = -391.51$ GeV, $\lambda_4 = 2.20$, $v_s = 276.21$ GeV, and $g_S = 0.056$. With these parameter setup, we obtain the correct DM relic density $\Omega h^2 = 0.121$, and DM annihilation cross section $\langle\sigma v\rangle = 2.26 \times 10^{-26} \text{ cm}^3 \text{ s}^{-1}$. The benchmark scenario can explain the Fermi gamma-ray

excess within the uncertainty of the galaxy halo profile near the GC like the other benchmark points. We discuss the collider signatures of the BP III in this subsection.

3.3.1 Higgs signal strength

The Higgs mixing angle $\sin \theta_s = 0.025$ corresponds to $\cos \theta_s = 0.9997$. It implies 0.03% reduction of hZZ coupling from the SM value. The future colliders including the ILC are not sensitive enough to measure such a small deviation.

3.3.2 Triple Higgs coupling

The triple Higgs coupling of the BP III is $c_{111} = 190.57$ GeV, which implies -0.15% deviation from the SM prediction. Such a small deviation will be very difficult to measure even in the 100 TeV pp collider.

3.3.3 Exotic Higgs decays

The singlet-like Higgs mass of the BP III ($m_{h_2} = 35.7$ GeV) is smaller than half of the SM-like Higgs mass, thus h_1 can decay into a new scalar pair h_2h_2 . The corresponding branching ratio is $\text{BR}(h_1 \rightarrow h_2h_2) = 7\%$. The light Higgs subsequently decays to mostly $b\bar{b}$, with $\text{BR}(h_2 \rightarrow b\bar{b}) = 86\%$, giving rise to $\text{BR}(h_1 \rightarrow h_2h_2 \rightarrow 4b) = 5.2\%$.

Recently, the ATLAS collaboration provided a result of search for the Higgs boson produced in association with a vector boson and decaying into two spin-zero particles in the $H \rightarrow aa \rightarrow 4b$ channel at the 13 TeV LHC with an integrated luminosity of 36.1 fb^{-1} [42]. The 95% C.L. upper limit on the combination of cross sections for WH and ZH times the branching ratio of $H \rightarrow aa \rightarrow 4b$ ranges from 3.0 pb for $m_a = 20$ GeV to 1.3 pb for $m_a = 60$ GeV. The upper limit is about 1.1 pb for $m_a = 35.7$ GeV. We can translate the result to an upper limit on the branching ratio $\text{BR}(h_1 \rightarrow h_2h_2 \rightarrow 4b) \lesssim 50\%$ with $m_{h_2} = 35.7$ GeV for the BP III, assuming the SM cross sections for WH and ZH . An order of improvement on the bound will be possible at the HL-LHC [43].

Searches for exotic Higgs decays with final states involving quarks are somewhat challenging at the LHC and HL-LHC. However, the ILC at $\sqrt{s} = 250$ GeV has an excellent sensitivity to search for such final states, due to low QCD backgrounds and the recoil mass technique for tagging the Higgs boson associated with the Z boson. Through the Higgsstrahlung process $e^+e^- \rightarrow Zh_1$ and the $h_1 \rightarrow h_2h_2 \rightarrow 4b$ decay, the 250 GeV ILC with the integrated luminosity of 2 ab^{-1} can exclude branching ratio of $h_1 \rightarrow h_2h_2 \rightarrow 4b$ down to $\sim 10^{-3}$ [44]. Therefore, we expect that the exotic Higgs decay of the BP III will be very well detected at the ILC experiment.

3.3.4 Production of h_2 at colliders

In the BP III, the Higgs mixing angle is $\sin^2 \theta_s = 6.25 \times 10^{-4}$ and the mass of the singlet-like Higgs is $m_{h_2} = 35.7$ GeV. Since the mixing angle value is much smaller than the ILC sensitivity given in Eq. (18), the signal for the $e^+e^- \rightarrow Zh_2$ process is beyond the reach of the ILC experiment.

	Higgs signal strength	Triple Higgs coupling	Exotic Higgs decay	h_2 production
BP I	0.7% reduction ○ ($\delta \sim 0.3\%$ (ILC))	3.9% reduction △ ($\delta \sim 4\%$ (FCC-hh))	$\text{BR}(h_1 \rightarrow \psi\bar{\psi}) = 0.73\%$ ○ ($\text{BR}(h \rightarrow \text{invisible}) \lesssim 0.3\%$ (ILC))	$m_{h_2} = 99.4 \text{ GeV}$, $\sin^2 \theta_s = 0.014$ ○ ($\sin^2 \theta_s \lesssim 0.0015$ (ILC))
BP II	0.6% reduction ○ ($\delta \sim 0.3\%$ (ILC))	22% reduction ○ ($\delta \sim 4\%$ (FCC-hh))	No exotic decay ×	$m_{h_2} = 213.5 \text{ GeV}$, $\sin^2 \theta_s = 0.012$ ○ ($\sin^2 \theta_s \lesssim 0.008$ (HL-LHC))
BP III	0.03% reduction ×	0.15% reduction ×	$\text{BR}(h_1 \rightarrow h_2 h_2) = 7\%$ ○ ($\text{BR}(h \rightarrow ss \rightarrow 4b) \lesssim 0.1\%$ (ILC))	$m_{h_2} = 35.7 \text{ GeV}$, $\sin^2 \theta_s = 6.3 \times 10^{-4}$ ×

Table 1: Summary of the collider signatures for the benchmark points. The circle (triangle) denotes that the collider signal of the benchmark can be (marginally) measurable at future colliders. The cases where the collider signal is expected to be hard to measure or beyond the reach of the future colliders are marked with the cross. The texts in parentheses are relevant bounds expected at the future colliders.

4 Conclusions

In this paper, we investigated various collider signatures of the three benchmark points in the SFDM model. The benchmark points were chosen to explain the Fermi gamma-ray excess at the GC from the DM pair annihilations in the previous study. According to the final state of the DM annihilation process, three benchmark points have been considered: DM annihilations into a pair of b quarks, SM-like Higgs bosons, and new scalars, dubbed as BP I, BP II, and BP III, respectively. The probe of such signals at colliders is necessary in order to either support or oppose the possibilities of explaining the gamma-ray excess in terms of the DM annihilation and the SFDM model is a proper reference model for that. We need a unique strategy to explore the signals of the each benchmark point, representing a parameter set of the DM annihilation channel providing a best fit to the observed excess. We categorize the search strategies by listing the four observables: Higgs signal strength, triple Higgs coupling, exotic Higgs decay, and production of the new scalar, h_2 , at future colliders such as ILC (easily convertible to CEPC as well), HL-LHC, and FCC-hh.

In Table 1, we briefly summarize the preferred observables to probe each benchmark point. It turns out that the BP I is expected to be explored by the measurements of the Higgs signal strength, exotic Higgs decay, and h_2 production at the ILC. As the triple Higgs coupling of the BP I is on the sensitivity limit of the FCC-hh, we expect that observing the deviation of the triple Higgs coupling will be marginally possible. All the collider observables except the exotic Higgs decay can probe the BP II. In particular, the triple Higgs coupling of the BP II is substantially smaller than the SM prediction. On the other hand, the BP III can be tested by the search for the exotic Higgs decay $h_1 \rightarrow h_2 h_2$. The direct production of h_2 is hardly measurable due to the small mixing angle. Since single collider observable is not sufficient to probe all the benchmark scenarios simultaneously, combined searches must be performed to find the new-physics signals at future lepton and hadron colliders.

Acknowledgments

We would like to thank Jia Liu, Zhen Liu, and Carlos Wagner for useful discussions. This work was performed in part at the Aspen Center for Physics, which is supported by National Science Foundation grant PHY-1607611. YGK is supported by the Basic Science Research Program through the National Research Foundation of Korea (NRF) funded by the Korean Ministry of Education, Science and Technology (NRF-2018R1D1A1B07050701). The work of CBP is supported by IBS under the project code, IBS-R018-D1. SS is supported by the National Research Foundation of Korea (NRF-2017R1D1A1B03032076). SS appreciates the hospitality of Fermi National Accelerator Laboratory.

References

- [1] L. Goodenough and D. Hooper, [arXiv:0910.2998](#) [hep-ph].
- [2] D. Hooper and L. Goodenough, Phys. Lett. B **697**, 412 (2011) [[arXiv:1010.2752](#) [hep-ph]].
- [3] D. Hooper and T. Linden, Phys. Rev. D **84**, 123005 (2011) [[arXiv:1110.0006](#) [astro-ph.HE]].
- [4] K. N. Abazajian and M. Kaplinghat, Phys. Rev. D **86**, 083511 (2012) [Phys. Rev. D **87**, 129902 (2013)] [[arXiv:1207.6047](#) [astro-ph.HE]].
- [5] D. Hooper and T. R. Slatyer, Phys. Dark Univ. **2**, 118 (2013) [[arXiv:1302.6589](#) [astro-ph.HE]].
- [6] C. Gordon and O. Macias, Phys. Rev. D **88**, no. 8, 083521 (2013) [Phys. Rev. D **89**, no. 4, 049901 (2014)] [[arXiv:1306.5725](#) [astro-ph.HE]].
- [7] W. C. Huang, A. Urbano and W. Xue, [arXiv:1307.6862](#) [hep-ph].
- [8] K. N. Abazajian, N. Canac, S. Horiuchi and M. Kaplinghat, Phys. Rev. D **90**, no. 2, 023526 (2014) [[arXiv:1402.4090](#) [astro-ph.HE]].
- [9] T. Daylan, D. P. Finkbeiner, D. Hooper, T. Linden, S. K. N. Portillo, N. L. Rodd and T. R. Slatyer, Phys. Dark Univ. **12**, 1 (2016) [[arXiv:1402.6703](#) [astro-ph.HE]].
- [10] F. Calore, I. Cholis and C. Weniger, JCAP **1503**, 038 (2015) [[arXiv:1409.0042](#) [astro-ph.CO]].
- [11] F. Calore, I. Cholis, C. McCabe and C. Weniger, Phys. Rev. D **91**, no. 6, 063003 (2015) [[arXiv:1411.4647](#) [hep-ph]].
- [12] M. Ajello *et al.* [Fermi-LAT Collaboration], Astrophys. J. **819**, no. 1, 44 (2016) [[arXiv:1511.02938](#) [astro-ph.HE]].
- [13] Y. G. Kim, K. Y. Lee, C. B. Park and S. Shin, Phys. Rev. D **93**, no. 7, 075023 (2016) [[arXiv:1601.05089](#) [hep-ph]].

- [14] Y. G. Kim, K. Y. Lee and S. Shin, JHEP **0805**, 100 (2008) [[arXiv:0803.2932](#) [hep-ph]].
- [15] Y. G. Kim and S. Shin, JHEP **0905**, 036 (2009) [[arXiv:0901.2609](#) [hep-ph]].
- [16] M. A. Fedderke, J. Y. Chen, E. W. Kolb and L. T. Wang, JHEP **1408**, 122 (2014) [[arXiv:1404.2283](#) [hep-ph]].
- [17] M. Ackermann *et al.* [Fermi-LAT Collaboration], Phys. Rev. Lett. **115**, no. 23, 231301 (2015) [[arXiv:1503.02641](#) [astro-ph.HE]].
- [18] O. Adriani *et al.* [PAMELA Collaboration], Phys. Rev. Lett. **105**, 121101 (2010) [[arXiv:1007.0821](#) [astro-ph.HE]].
- [19] M. Aguilar *et al.* [AMS Collaboration], Phys. Rev. Lett. **117**, no. 9, 091103 (2016).
- [20] K. Fujii *et al.*, [arXiv:1506.05992](#) [hep-ex].
- [21] J. Liu, X. P. Wang and F. Yu, JHEP **1706**, 077 (2017) [[arXiv:1704.00730](#) [hep-ph]].
- [22] K. Fujii *et al.*, [arXiv:1710.07621](#) [hep-ex].
- [23] S. Di Vita, G. Durieux, C. Grojean, J. Gu, Z. Liu, G. Panico, M. Riembau and T. Vantalón, JHEP **1802**, 178 (2018) [[arXiv:1711.03978](#) [hep-ph]].
- [24] CMS Collaboration, [arXiv:1307.7135](#) [hep-ex].
- [25] ATLAS Collaboration, ATL-PHYS-PUB-2014-016.
- [26] ATLAS collaboration, ATL-PHYS-PUB-2017-001.
- [27] H. J. He, J. Ren and W. Yao, Phys. Rev. D **93**, no. 1, 015003 (2016) [[arXiv:1506.03302](#) [hep-ph]].
- [28] R. Contino *et al.*, CERN Yellow Report, no. 3, 255 (2017) [[arXiv:1606.09408](#) [hep-ph]].
- [29] T. Barklow, K. Fujii, S. Jung, R. Karl, J. List, T. Ogawa, M. E. Peskin and J. Tian, Phys. Rev. D **97**, no. 5, 053003 (2018) [[arXiv:1708.08912](#) [hep-ph]].
- [30] ATLAS Collaboration, ATL-PHYS-PUB-2013-014.
- [31] CMS Collaboration, CMS-PAS-HIG-17-013.
- [32] D. Liu, J. Liu, C. E. M. Wagner and X. P. Wang, JHEP **1806**, 150 (2018) [[arXiv:1805.01476](#) [hep-ph]].
- [33] ALEPH and DELPHI and L3 and OPAL Collaborations and LEP Working Group for Higgs boson searches, Phys. Lett. B **565**, 61-75 (2003) [[arXiv:hep-ex/0306033](#)].
- [34] J. Alwall *et al.*, JHEP **1407**, 079 (2014) [[arXiv:1405.0301](#) [hep-ph]].
- [35] P. Drechsel, G. Moortgat-Pick, and G. Weiglein, [arXiv:1801.09662](#) [hep-ph].
- [36] Y. Wang, J. List and M. Berggren, [arXiv:1801.08164](#) [hep-ex].

- [37] CMS Collaboration, JHEP **1510** (2015) 144 [[arXiv:1504.00936](#) [hep-ex]].
- [38] ATLAS Collaboration, Eur. Phys. J. C **78** (2017) no. 4, 293 [[arXiv:1712.06386](#) [hep-ex]].
- [39] CMS Collaboration, JHEP **1806** (2018) 127 [[arXiv:1804.01939](#) [hep-ex]].
- [40] CMS Collaboration, CMS-PAS-FTR-13-024.
- [41] B. Dutta, Y. Gao, T. Ghosh, and L. E. Strigari, Phys. Rev. D **92** (2015) no.7, 075019 [[arXiv:1508.05989](#) [hep-ph]].
- [42] M. Aaboud *et al.* [ATLAS Collaboration], [arXiv:1806.07355](#) [hep-ex].
- [43] D. Curtin *et al.*, Phys. Rev. D **90**, no. 7, 075004 (2014) [[arXiv:1312.4992](#) [hep-ph]].
- [44] Z. Liu, L. Wang and H. Zhang, Chinese Physics C Vol. 41, No. 6 (2017) 063102 [[arXiv:1612.09284](#) [hep-ph]].